Characterization of Thermomechanical Behavior of Ti3SiC2 and Ti2AlC Ceramics Elaborated by Spark Plasma Sintering Using Ultrasonic Means

Karolina Kozak, Ariane Dosi, Guy Antou, Nicolas Pradeilles, Thierry Chotard

Characterization of Thermomechanical Behavior of Ti_3SiC_2 and Ti_2AlC Ceramics Elaborated by Spark Plasma Sintering Using Ultrasonic Means**

By Karolina Kozak,* Ariane Dosi, Guy Antou,* Nicolas Pradeilles and Thierry Chotard*

In order to better understand the thermomechanical behaviors of Ti3SiC2 and Ti2AlC ceramics, sintered by spark plasma sintering process (SPS), ultrasonic pulse echography in "long bar mode" (US) and acoustic emission (AE) techniques are applied. High-temperature investigations of the evolution of Young's modulus (E) and AE activity are carried out up to 1 473 and 1 623 K. Results show a decrease of E with increasing temperature which is more marked around maximal temperature of the thermal cycle for Ti2AlC material. Moreover, the increase of the maximal temperature of the thermal cycle influences the number of recorded cumulated hits. Both measurements (US þ AE) highlight the role of the plastic deformation mechanism (motion of dislocation) activated over the brittle-to-plastic transition temperature.

1. Introduction

$M_{n+1}AX_n$ phases (with $n = 1$, 2, or 3) form a class of nano-laminated ternary carbides or nitrides, with a hexagonal structure, where M is an early transition metal, A is an A-group element, and X is either carbon or nitrogen. In these materials, the $M_{n+1}AX_n$ layers, characterized by mostly strong covalent M–X bonds, are interleaved with A layers through weak M–A bonds. This inherent nano-layered structure provides a unique combination of metal-like and ceramic-like properties. The metal-like part refers to their good thermal and electrical conductivity, easy machinability with conventional tools, and good resistance to thermal shocks. Like ceramics, these materials have high melting temperature, high strength, good wear and corrosion resistance, and are stable up to elevated temperatures.[1,2] Because of these unique properties mentioned above, it is expected to apply in various fields, such as structural material for high temperature, refractory material thanks to good thermal shock resistance, substitute for machinable ceramics,[3] bioceramic composites, thanks to biocompatibility,[4] neutron irradiation resistant parts for nuclear applications.[5]

From all known materials from this group, Ti_3SiC_2 and Ti_2AlC have gained the greatest interest. Both of them are considered as good candidates for high-temperature applications due to their excellent fatigue and creep resistance.[6,7] Nowadays, both of them can be synthesized by several methods like Self-propagating High-temperature Synthesis (SHS) firstly reported by Pampuch et al.[8] reactive Hot Isostatic Pressing (HIP) reported by Gao et al. and Radovic et al.[9,10] Recently, a great attention is addressed toward a non-conventional technique named Spark Plasma Sintering (SPS). In 2005, Zhou et al. have reported that fully dense Ti_3SiC_2 and Ti_2AlC samples with fine microstructure are possible to obtain via this method thanks to high heating rates (of a few hundred K min^{-1}).[3,11] Synthesis of pure single-phase Ti_3SiC_2 is difficult, and depends on starting powders. The most common impurities coexisting with Ti_3SiC_2 are TiC, SiC, and Ti_xSi_y.[12,13] In case of Ti_2AlC compound, possible secondary phases are Ti_3AlC_2, $Ti_xAl_{y,}$ and TiC_x.[14,15]

[*] *K. Kozak, Dr. G. Antou, Prof. Dr. T. Chotard, A. Dosi, N. Pradeilles*
Université de Limoges, SPCTS, UMR 7315, F-87000 Limoges, France
E-mail: karolina.kozak@etu.unilim.fr; guy.antou@unilim.fr; thierry.chotard@unilim.fr
K. Kozak
AGH University of Science and Technology, Faculty of Materials Science and Ceramics, al. Mickiewicza 30, 30-059 Kraków, Poland

[**] *The authors would like to acknowledge M. Vandenhende from SPCTS laboratory for the help in carrying out SPS experiments. They also want to thank the French Ministry of Foreign Affairs and the University AGH of Krakow (Poland) for funding the scholarship of the co-supervised PhD thesis of Miss Kozak. The authors report no financial or other conflict of interest relevant to the subject of this article.*

In the literature, several works have already been conducted to study the mechanical properties of the MAX phases and to understand the involved deformation mechanisms.[6,10,16–18] Standard stress-strain curves exhibit a reversible nonlinear behavior during loading cycles.[19,20] This fact leads to a significant deformation to rupture. Based on TEM observations, Barsoum et al. suggest, that, under mechanical stress, this reversible nonlinear behavior might be explained by the occurrence and annihilation of Incipient Kink Bands (IKBs).[17,21] When the stress reaches a critical value, IKBs transform into stable Kink Bands (KBs). Formation of those requires a generation of several regularly spaced dislocation pairs on several parallel slip planes. Moreover, at high temperatures (>1 173 K), MAX phases undergo brittle-to-plastic transition (BPT) increasing therefore possible deformation to rupture.[6]

The main aim of this work is to investigate, thanks to ultrasonic means (i.e., US pulse echography (US) and Acoustic Emission (AE)), the thermomechanical behavior of such materials, and to characterize their possible microstructural changes during heating and cooling stages helped by AE activity recording and analysis.

2. Materials and Methods

2.1. Materials Elaboration by Spark Plasma Sintering (SPS)

Two commercially available raw powders were used (Maxthal 312 and Maxthal 211 for Ti_3SiC_2 and Ti_2AlC, respectively, KANTHAL Company, Sweden). The Ti_3SiC_2 and Ti_2AlC powders exhibit a quite monodisperse distribution in volume with average sizes of $9.4 \pm 1.5\,\mu m$ and $11.5 \pm 0.1\,\mu m$, respectively (measured by laser granulometry, AccuPyc II 1340 apparatus, Micrometrics France S.A. Verneuil Halatte, France).

The powders were densified without sintering additives by SPS technique. The SPS apparatus was used is a Dr. Sinter 825 (Fuji Electronics Industrial Co. Ltd., Japan). The powders were poured into a graphite die with an internal diameter of 50.4 mm. Sintered specimens had the thickness of 5 mm. A compressible graphite foil (0.2 mm thick, Papyex, Mersen, France) was used as lubricant to coat the inner surface of the die and the surface of the punches. The die was covered by a graphite felt in order to reduce the heat radiation, and hence radial thermal gradients during sintering. The sintering cycles were carried out in vacuum. For Ti_3SiC_2 powder, the heating rate was $100\,K\,min^{-1}$ up to 1 523 K, with a dwell of 5 min. For Ti_2AlC powder, the heating rate was $100\,K\,min^{-1}$ up to 1 423 K, with a dwell of 5 min. In both cases, a uniaxial pressure of 75 MPa was applied during the heat treatment, and a controlled cooling rate of $25\,K\,min^{-1}$ was applied down to 1 473 K, in order to reduce quenching stresses.

2.2. Microstructural and Structural Analysis

The final densities of sintered samples were determined using the Archimede's method with deionized water. Five measurements were made for each sample.

Microstructural observations were performed by SEM with a JSM-7400 microscope (JEOL Ltd., Japan).

Phase identification of bulk-sintered materials were carried out with a D5000 Siemens (Munich, Germany) X-ray diffractometer (40 kV, 30 mA, $CuK\alpha_1$ radiation). 2θ scanning step of 0.03° and a step time of 15 s was used in the range of $5° < 2\theta < 100°$.

2.3. Thermomechanical Characterization

Elastic constants (Young's modulus, shear modulus) were determined at room temperature by ultrasonic pulse echography in "infinite mode," using 10 MHz transducers working in reflection mode (WC37-10 and SW37-10, Ultran, State College, USA) on 4 mm thick samples.

The evolution of Young's modulus with temperature was carried out by high-temperature ultrasonic pulse echography in "long bar mode." This technique permits to follow, in a continuous way, changes in value of this elastic constant while temperature increases or decreases. The configuration of this technique and equation used to calculate the Young's modulus values are presented elsewhere.[22] The uncertainness of the US measurement ranges between 2 and 5%. For this measurement, dimensions of the rectangular samples were $40 \times 2 \times 2\,mm^3$. The working frequency was 300 kHz. Both materials were submitted to the following thermal cycle: i) heating rate of $5\,K\,min^{-1}$ up to 1 623 K; ii) dwell of 30 min; and iii) cooling stage at $5\,K\,min^{-1}$ down to room temperature.

AE technique is devoted to the in situ investigation and characterization of the evolution of the material's microstructure submitted to stress (mechanical, thermal, etc.). In case of solid materials, microstructural changes like dislocations slip, plastic deformation of grains, grains boundaries sliding, and cracks formations and propagations are sources of elastic waves.[23–25] These rapid releases of energy are detected and recorded in real-time in order, through the established chronology of events, to characterize and identify the specific involved mechanisms. Samples were prepared with standard machining tools and had dimensions of $25 \times 4 \times 4\,mm^3$. In this study, AE activity was recorded for both materials during two successive thermal cycles here defined: i) heating rate of $5\,K\,min^{-1}$ up to 1 473 K or 1 623 K; ii) dwell time of 30 min; iii) cooling rate of $5\,K\,min^{-1}$ down to 343 K. Experimental setup for high-temperature AE measurements and features extracted from recorded signals are described elsewhere.[22] In order to avoid oxidation of samples, both ultrasonic pulse echography and AE measurements were conducted in Argon atmosphere.

3. Results

3.1. Microstructure of Sintered Samples

For both compounds, the optimized SPS conditions allow obtaining samples with relative densities higher than 99%. SEM observations revealed a laminated structure characterized by the presence of elongated grains with width of 2–5 μm and length of 10–15 μm whose longer axis is perpendicular to

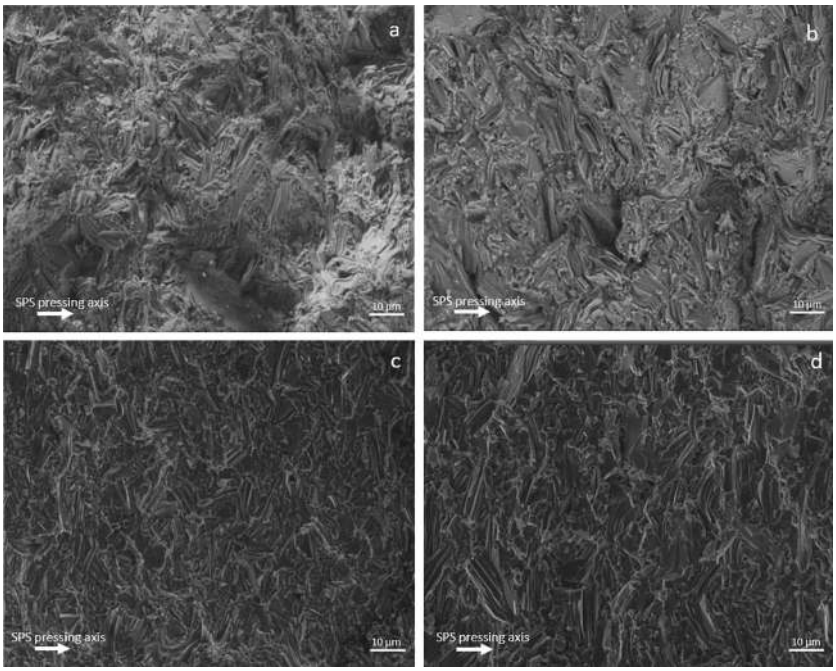

Fig. 1. SEM observations of sintered ceramics after SPS process (a: Ti_3SiC_2 and b: Ti_2AlC), and after thermal treatment at maximum temperature of 1 623 K (c: Ti_3SiC_2 and d: Ti_2AlC).

the direction of applied load during SPS treatment (Figure 1a and b).

Figure 2 shows XRD patterns of both Ti–Si–C and Ti–Al–C sintered ceramics respectively. In Ti–Si–C sample, Ti_3SiC_2 (considered as MAX phase), TiC and $TiSi_2$ (both here considered as impurities) phases are identified after sintering at 1 523 K and they still remain after thermal cycle during AE recording up to 1 623 K. In the literature, the smaller spherical grains observed by SEM are attributed to TiC and $TiSi_2$ secondary phases.[3] In Ti–Al–C sample, Ti_3AlC_2 and Ti_2AlC MAX phases are present after sintering at 1 423 K and stay after AE measurement up to 1 623 K. It is important to notice that no secondary phases which could be considered as impurities are present. We will see later in the paper that this observation is of prime importance when interpreting AE outputs.

3.2. Thermomechanical Properties

3.2.1. Elastic Properties at Room Temperature

The measured elastic constants by ultrasonic method were: i) for Ti_3SiC_2 ceramic, Young's (E), and shear (G) moduli, respectively of 335 ± 2 GPa and 141 ± 2 GPa leading to a Poisson's ratio (ν) of 0.186 ± 0.009; ii) for Ti_2AlC ceramic, E and G moduli, respectively of 282 ± 2 GPa and 119 ± 2 GPa leading to a ν of 0.185 ± 0.009. The measured elastic values are very close to the ones obtained in the literature.[26]

3.2.2. Thermomechanical Behavior

Figure 3 presents the continuous evolution of E versus temperature for both investigated compositions. For Ti_3SiC_2 material (solid line), when the temperature increases, value of E decreases linearly with a slope of $0.058\ GPa\ K^{-1}$. In turn, at the beginning of the cooling stage, a stiffening of the material is observed. In case of the Ti_2AlC material (dotted line), the obtained curve can be divided into two parts. Up to 1 523 K, as for Ti_3SiC_2, E value decreases linearly with increasing temperature (slope of $0.041\ GPa\ K^{-1}$). When reaching 1 523 K, E declines more rapidly with corresponding slope of $0.093\ GPa\ K^{-1}$. Hardening of the material while cooling is significantly less marked than for Ti_3SiC_2.

Differences in behavior between Ti_3SiC_2 and Ti_2AlC compounds revealed by US measurements, led us to check materials AE activity when the maximal temperature of the thermal cycle changes. Figure 4 presents results of AE

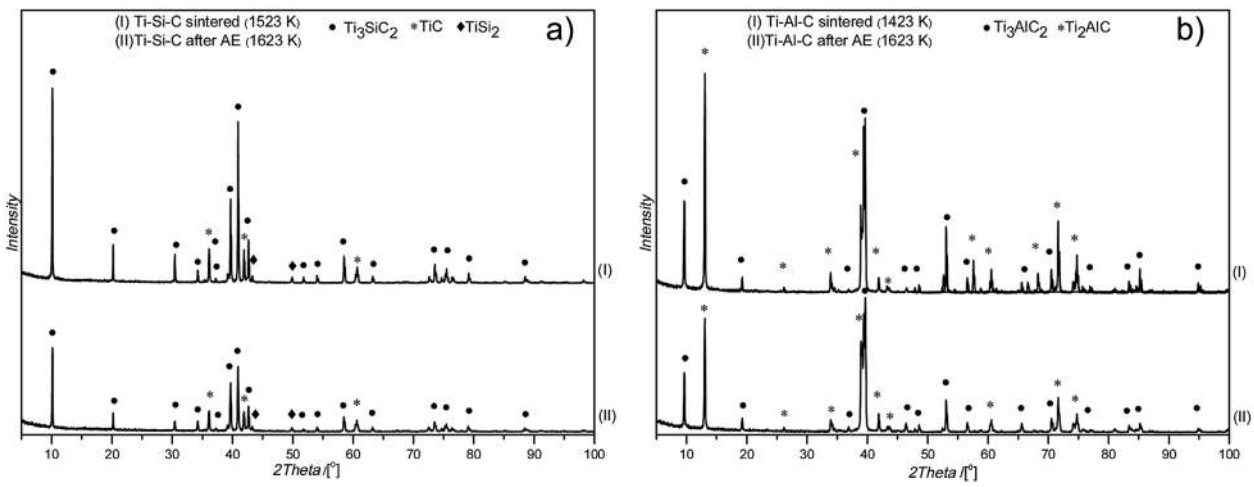

Fig. 2. XRD patterns of sintered materials: (a) Ti_3SiC_2 and (b) Ti_2AlC.

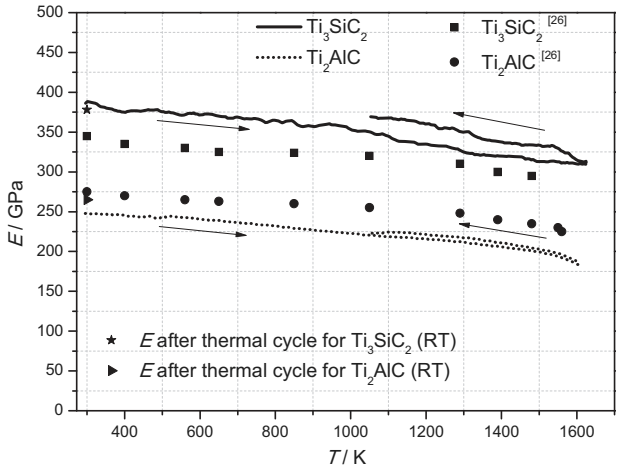

Fig. 3. Evolution of Young's modulus versus temperature for Ti_3SiC_2 and Ti_2AlC materials.

measurements for Ti_3SiC_2 (solid line) and Ti_2AlC (dotted line) during thermal treatments up to 1 473 and 1 623 K.

For both materials, it is important to state that the majority of records occurs during the cooling stage. Considering Ti_3SiC_2 material, it can be noticed that increasing the maximum temperature of the thermal cycle does not change the number of acoustic records. In opposite, for Ti_2AlC compound, the AE activity strongly increases (ten times higher): from ≈200 recorded cumulated hits after two cycles at 1 473 K to ≈2 000 ones after two cycles up to 1 623 K. This significant difference obviously reveals a microstructural change within the Ti_2AlC material for this shift in temperature.

4. Discussion

Both experimental ultrasonic techniques implemented in this work allow investigating, in a deeper way, the thermomechanical behavior of such materials. The obtained results will make possible after coupled analysis, to propose, in a quantitative and qualitative manner, some interpretations leading to a better understanding of the chronology of the suggested involved mechanisms at microstructural scale.

The US in "long bar mode" made possible to investigate continuously the evolution of Young's modulus versus temperature. For both ternary compounds, E values tend to decrease when the temperature increases reaching 1 623 K. Similar investigations were carried out by Radovic,[26] implementing resonant ultrasound spectroscopy (RUS) method, for Ti_3SiC_2 and Ti_2AlC between 298 and 1 573 K. For Ti_3SiC_2, results presented here are in good agreement with values obtained by RUS method which show a linear decrease of E when the temperature increases, with an estimated slope of 0.045 GPa K^{-1}. For Ti_2AlC, Radovic et al. did not notice any difference in tendency when temperature reaches 1 523 K: for the whole temperature range, E decreases linearly with a slope of 0.039 GPa K^{-1}. Values of E measured by US are lower for Ti_3SiC_2 and higher for Ti_2AlC than those measured with RUS method. Two reasons are possible to explain the differences between Radovic's measurements and those presented here: firstly, the difference in grain size; secondly, the difference in experimental conditions, anisothermal ultrasonic recording in this study contrary to isothermal for Radovic. However, we noticed a greater decrease of E above 1 523 K for Ti_2AlC material. The continuous mode of US recording versus temperature allows to accurately detect the change in mechanical behavior.

Based on US results, the behavior of both materials was more deeply investigated when the maximum temperature reaches 1 473 or 1 623 K (Figure 4). It is important to noticed that no change of the microstructure neither the grain size of both materials were observed after these thermal treatments (Figure 1c and d). The chosen maximal temperatures of the thermal cycles correspond to the temperature range when the slope of the curve E versus temperature drops significantly for Ti_2AlC.

Comparing AE activity of both materials up to 1 473 K, the one of Ti_3SiC_2 is two time higher than the Ti_2AlC one.

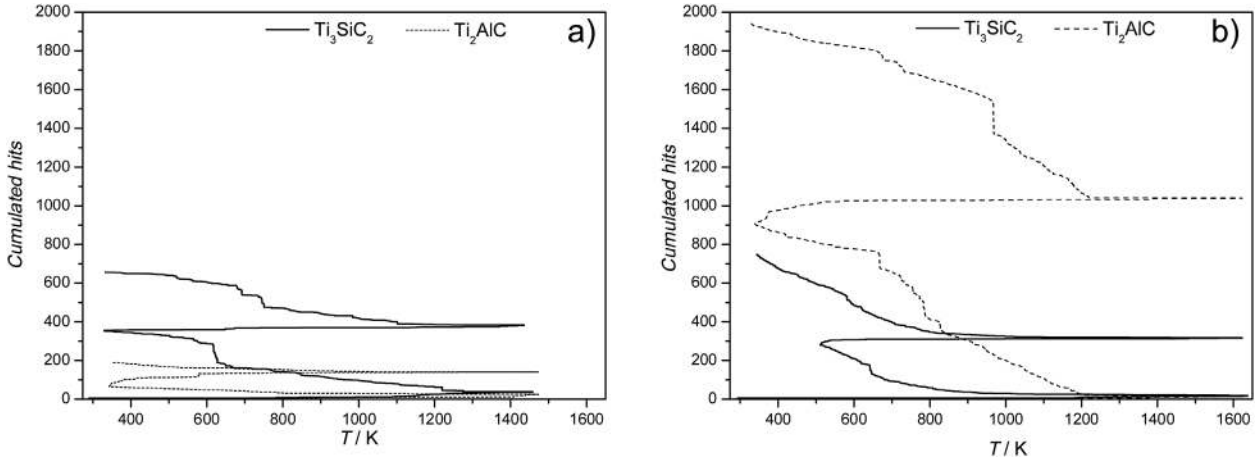

Fig. 4. AE activity versus temperature for both materials during thermal cycles up to: (a) 1 473, (b) 1 623 K.

Considering a zero stress-state at maximum temperature, higher level of AE activity for Ti_3SiC_2 up to 1 473 K could be related to: i) higher thermal strains induced during cooling considering the difference in thermal expansion coefficient, that is, $9.3 \times 10^{-6} K^{-1}$ for Ti_3SiC_2 and $7.9 \times 10^{-6} K^{-1}$ for Ti_2AlC;[27,28] ii) the presence of impurities (i.e., TiC and $TiSi_2$ as detected by XRD analysis) for Ti_3SiC_2, in contrary to Ti_2AlC, that leads to thermal expansion mismatch between phases constituting the material.

As mentioned in the paragraph 3.2.2, AE of Ti_3SiC_2 is comparable for thermal cycle at both maximum temperatures (i.e., 1 473 and 1 623 K). It could be concluded that, for this shift of the maximal temperature, no additional deformation mechanisms, or damage accumulation process are activated. In case of Ti_2AlC, the increased temperature influences significantly the number of recorded hits. Considering the work of Benitez on Ti_2AlC material under cyclic compressive loading, one could easily relate the presence of impurities ($TiAl_x$, Al_2O_3, TiC, 5 vol% in amount) with the possible occurrence of microcracking process due to elastic property mismatch between phases.[20] The obvious fact of no detection of impurity in our Ti_2AlC material, leads us to another hypothesis of interpretation concerning AE results. For Ti_2AlC, the sudden occurrence of large amount of hits, almost ten times higher for 1 623 K cycle than for 1 473 K cycle, is correlated to the evolution of the ultrasonic measurements for Young's modulus. Indeed, for this compound and according to literature data,[1,6,7] reaching 1 623 K means that the brittle-to-plastic transition is largely overshot. This fact is correlated with: i) the drop of the slope of the Young's modulus versus temperature curve, that is, $0.041\,GPa\,K^{-1}$ up to 1 523 K and $0.093\,GPa\,K^{-1}$ from 1 523 to 1 623 K, which points out a loss of rigidity in the interatomic bonds; ii) the attenuation of the US and AE signals at high temperature, which suggests the activation of viscoplasticity phenomenon affecting the material. The overcoming of the BPT may cause the activation of viscoplastic deformation mechanisms. As shown by Radovic et al. during tensile creep tests, the dominant viscoplastic mechanism is associated with dislocation creep, and is characterized by generation and dissipation of large internal stresses generated by the high plastic anisotropy of MAX phases.[6] This induces the sudden release of energy in the microstructure illustrated by the significant difference observed in AE activity (ten times higher).

5. Conclusions

The thermomechanical properties of Ti_3SiC_2 and Ti_2AlC ceramics were characterized and correlated to their chemical composition, structure, and microstructure. For Ti_3SiC_2 and Ti_2AlC, SPS sintering temperatures of 1 523 and 1 423 K, respectively are well-optimized giving bulk samples with more than 99% of relative density.

US in "infinite mode" confirms higher rigidity of Ti_3SiC_2 (335 ± 2 GPa) than Ti_2AlC (282 ± 2 GPa) being in good agreement with literature data.

US in "long bar more" between 298 and 1 623 K revealed decreasing temperature dependency of E for both materials. Above ≈1 523 K, the slope of the E versus temperature curve for Ti_2AlC drops more rapidly, highlighting the overcoming of the BPT for this compound. The consequences are observed in AE activity by a raise of the cumulated hits number during cooling stage. It might be explained by activation of plastic deformation mechanisms when Ti_2AlC undergoes brittle-to-plastic transition.

In order to better understand the mechanical response of MAX phases, four-point bending test coupled with AE facilities will be carried out in a next study.

[1] M. W. Barsoum, M. Radovic, in *Encycl. Mater. Sci. Technol. Second Ed*. (Ed: K. H. J. B. W. C. C. F. I. J. K. M. Veyssière), Elsevier, Oxford **2004**, 1.

[2] M. W. Barsoum, M. Radovic, *Annu. Rev. Mater. Res*. **2011**, *41*, 195.

[3] W. B. Zhou, B. C. Mei, J. Q. Zhu, *Mater. Lett*. **2005**, *59*, 1547.

[4] M. A. El Saeed, F. A. Deorsola, R. M. Rashad, *Int. J. Refract. Met. Hard Mater*. **2013**, *41*, 48.

[5] D. J. Tallman, E. N. Hoffman, E. N. Caspi, B. L. Garcia-Diaz, G. Kohse, R. L. Sindelar, M. W. Barsoum, *Acta Mater*. **2015**, *85*, 132.

[6] M. Radovic, M. W. Barsoum, T. El-Raghy, S. M. Wiederhorn, *J. Alloys Compd*. **2003**, *361*, 299.

[7] M. Radovic, M. W. Barsoum, T. El-Raghy, S. Wiederhorn, *Acta Mater*. **2001**, *49*, 4103.

[8] R. Pampuch, J. Lis, L. Stobierski, M. Tymkiewicz, *J. Eur. Ceram. Soc*. **1989**, *5*, 283.

[9] N. F. Gao, Y. Miyamoto, D. Zhang, *Mater. Lett*. **2002**, *55*, 61.

[10] M. Radovic, M. W. Barsoum, T. El-Raghy, J. Seidensticker, S. Wiederhorn, *Acta Mater*. **2000**, *48*, 453.

[11] W. B. Zhou, B. C. Mei, J. Q. Zhu, X. L. Hong, *Mater. Lett*. **2005**, *59*, 131.

[12] N. F. Gao, J. T. Li, D. Zhang, Y. Miyamoto, *J. Eur. Ceram. Soc*. **2002**, *22*, 2365.

[13] T. L. Ngai, Y. Kuang, Y. Li, *Ceram. Int*. **2012**, *38*, 463.

[14] S.-B. Li, H.-X. Zhai, G.-P. Bei, Y. Zhou, Z.-L. Zhang, *Ceram. Int*. **2007**, *33*, 169.

[15] V. Gauthier-Brunet, T. Cabioc'h, P. Chartier, M. Jaouen, S. Dubois, *J. Eur. Ceram. Soc*. **2009**, *29*, 187.

[16] M. W. Barsoum, in *MAX Phases*, Wiley-VCH Verlag GmbH & Co. KgaA **2013**, 307.

[17] M. W. Barsoum, T. Zhen, S. R. Kalidindi, M. Radovic, A. Murugaiah, *Nat. Mater*. **2003**, *107*, 2.

[18] R. Bhattacharya, R. Benitez, M. Radovic, N. C. Goulbourne, *Mater. Sci. Eng. A* **2014**, *598*, 319.

[19] N. G. Jones, C. Humphrey, L. D. Connor, O. Wilhelmsson, L. Hultman, H. J. Stone, F. Giuliani, W. J. Clegg, *Acta Mater*. **2014**, *69*, 149.

[20] R. Benitez, W. H. Kan, H. Gao, M. O'Neal, G. Proust, M. Radovic, *Acta Mater.* **2016**, *105*, 294.
[21] I. L. L. Farber, *Philos. Mag. Lett*. **1999**, *163*, 79.
[22] G. Briche, N. Tessier-Doyen, M. Huger, T. Chotard, *J. Eur. Ceram. Soc*. **2008**, *28*, 2835.
[23] D. Bianchi, E. Mayrhofer, M. Gröschl, G. Betz, A. Vernes, *Mech. Syst. Signal Process*. **2015**, *64–65*, 441.
[24] L. H. A. Maia, A. M. Abrao, W. L. Vasconcelos, W. F. Sales, A. R. Machado, *Tribol. Int*. **2015**, *92*, 519.
[25] A. Vinogradov, I. S. Yasnikov, *Acta Mater.* **2014**, *70*, 8.
[26] M. Radovic, M. W. Barsoum, A. Ganguly, T. Zhen, P. Finkel, S. R. Kalidindi, E. Lara-Curzio, *Acta Mater.* **2006**, *54*, 2757.
[27] T. Zhen, M. W. Barsoum, S. R. Kalidindi, *Acta Mater.* **2005**, *53*, 4163.
[28] Y. Bai, H. Zhang, X. He, C. Zhu, R. Wang, Y. Sun, G. Chen, P. Xiao, *Int. J. Refract. Met. Hard Mater.* **2014**, *45*, 58.